Cell Death and Differentiation (2008) 15, 1318–1329

www.nature.com/cdd

Role of non-canonical Beclin 1-independent autophagy in cell death induced by resveratrol in human breast cancer cells

F Scarlatti[1,3], R Maffei[1], I Beau[2], P Codogno*[,2,4] and R Ghidoni*[,1,4]

Resveratrol, a polyphenol found in grapes and other fruit and vegetables, is a powerful chemopreventive and chemotherapeutic molecule potentially of interest for the treatment of breast cancer. The human breast cancer cell line MCF-7, which is devoid of caspase-3 activity, is refractory to apoptotic cell death after incubation with resveratrol. Here we show that resveratrol arrests cell proliferation, triggers death and decreases the number of colonies of cells that are sensitive to caspase-3-dependent apoptosis (MCF-7^{casp-3}) and also those that are unresponsive to it (MCF-7^{vc}). We demonstrate that resveratrol (i) acts via multiple pathways to trigger cell death, (ii) induces caspase-dependent and caspase-independent cell death in MCF-7^{casp-3} cells, (iii) induces only caspase-independent cell death in MCF-7^{vc} cells and (iv) stimulates macroautophagy. Using *BECN1* and *hVPS34* (human vacuolar protein sorting 34) small interfering RNAs, we demonstrate that resveratrol activates Beclin 1-independent autophagy in both cell lines, whereas cell death via this uncommon form of autophagy occurs only in MCF-7^{vc} cells. We also show that this variant form of autophagic cell death is blocked by the expression of caspase-3, but not by its enzymatic activity. In conclusion, this study reveals that non-canonical autophagy induced by resveratrol can act as a caspase-independent cell death mechanism in breast cancer cells.
Cell Death and Differentiation (2008) **15,** 1318–1329; doi:10.1038/cdd.2008.51; published online 18 April 2008

Macroautophagy (hereafter referred to as autophagy) is an evolutionarily conserved catabolic pathway in which cytoplasmic components are sequestered in vacuoles known as autophagosomes, where they undergo bulk lysosomal degradation.[1,2]

Autophagy is a cytoprotective mechanism that protects cells exposed to situations of metabolic stress, such as nutrient deprivation.[2] Autophagosome formation is dependent on the activity of Atg proteins, evolutionarily conserved from yeast to humans.[3] Of these Atg proteins, the Beclin 1 complex (Beclin 1 is the mammalian ortholog of yeast Atg-6) and two ubiquitin-like conjugation systems, the Atg12 and light chain 3 (LC3) systems (LC3 is the mammalian ortholog of yeast Atg8), act sequentially during the nucleation and expansion of the autophagosomal membrane.

The 'autophagic cell death' is a form of programmed cell death,[4] morphologically distinct from apoptosis and characterized by the accumulation of autophagic vacuoles. Many cancer chemotherapies and radiation are potent inducers of autophagy.[5]

Resveratrol (Res), a polyphenol found in grapes, peanuts and other plants, has potent antioxidant and antitumorigenic activities,[6] affects tumor initiation and promotion, and arrests angiogenesis and metastasis. It is also able to stimulate apoptosis, arrest cell cycle and suppress kinase pathways.[7] Res promotes cell death in ovarian carcinoma cells by triggering both autophagy and apoptosis.[8]

Additionally, Res inhibits tumor formation in animal models of carcinogenesis.[9,10] Phase-I human clinical trials of oral Res are currently in progress.[11]

Resistance to apoptotic stimuli has been attributed to MCF-7 human breast carcinoma cells. These cells lack caspase-3, due to a 47-base-pair deletion within exon 3 of the caspase-3 gene.[12] Curiously, this cell line is sensitive to Res, although its action cannot be mediated by either caspase-3, which is absent, or by caspase-8, which is unaffected.[13] Nevertheless, the effects of Res on breast cancer MCF-7 cell lines are controversial. Indeed, other studies have demonstrated the occurrence of chromatin condensation and activation of caspase-9 in MCF-7 cells following exposure to Res.[14,15]

[1]Laboratory of Biochemistry and Mol Biology, San Paolo University Hospital, Medical School, University of Milan, Milan, Italy; [2]INSERM U756, Université Paris-Sud 11, Châtenay-Malabry, France and [3]Laboratory of Cellular and Molecular Endocrinology, Division of Endocrinology and Metabolism, Department of Internal Medicine, University of Turin, Turin, Italy
*Corresponding authors: R Ghidoni, Laboratory of Biochemistry and Mol Biology, San Paolo University Hospital, Medical School, University of Milan, Via di Rudiní, 8, Milan 20142, Italy.
Tel: +39 02 503 232 50; Fax: +39 02 503 232 45;
E-mail: riccardo.ghidoni@unimi.it and
P Codogno, INSERM U756, Faculté de Pharmacie, Université Paris-Sud 11, 92296 Châtenay-Malabry, France.
Tel: +33 146835720; Fax: +33 146835844; E-mail: patrice.codogno@u-psud.fr
[4]These authors should be regarded as senior authors.
Keywords: macroautophagy; caspase-independent cell death; apoptosis; necrosis
Abbreviations: Res, resveratrol; ATG, autophagy-related genes; C_2-Cer, C_2-ceramide; GFP, green fluorescent protein; LC3, light chain 3; 3-MA, 3-methyladenine; Vps34, vacuolar protein sorting 34; PBS, phosphate-buffered saline; siRNA, small interfering RNA; PIC, protease inhibitor mixture; PARP, poly(ADP-ribose) polymerase; PI, propidium iodide; Pep A, pepstatin A; Ac-DEVD-pNA, acetyl-Asp-Glu-Val-Asp *p*-nitroanilide; PKB, protein kinase B; PI3K, phosphoinositide 3-kinase
Received 29.8.07; revised 12.3.08; accepted 17.3.08; Edited by E Baehrecke; published online 18.4.08

In this study, we investigate the mechanism by which Res induces death in cells that are sensitive or refractory to apoptosis. To this end, we used a cell model involving both caspase-3-competent (MCF-7^{casp-3}) and caspase-3-incompetent (MCF-7^{vc}) cells. Our findings show that Res induces both caspase-dependent and caspase-independent cell death, with clearly evident necrotic features in MCF-7^{casp-3} cells. In MCF-7^{vc}, caspase-independent cell death alone occurs in response to Res treatment. Interestingly, Res induces Beclin 1-independent autophagy in both cell populations, as demonstrated by a lack of sensitivity of autophagic markers (LC3-II accumulation, punctate green fluorescent protein (GFP)-LC3 structures, 3-methyladenine (3-MA)-sensitive proteolysis) to *BECN1* (Beclin 1) and *hVPS34* (human vacuolar protein sorting 34) small interfering RNA (siRNAs). This non-canonical autophagy forms part of the caspase-independent cell death process in MCF-7^{vc} cells, but not in MCF-7^{casp-3} cells.

In conclusion, Res kills cancer cells via several different pathways. Moreover, Res reveals that a novel type of autophagy can be activated in breast cancer cells, which bypasses the activity of tumor suppressor Beclin 1. Finally, the Res-induced autophagic cell death is blocked by the expression of caspase-3, but not by its enzymatic activity.

Results

Res inhibits proliferation and promotes cell death regardless of caspase-3 expression. The biological effects of Res in MCF-7 cells were investigated to determine proliferation index, loss of viability and number of colonies. Res inhibited MCF-7 cell proliferation in a time- and dose-dependent manner, with an efficacy that was unrelated to caspase-3 expression (Figure 1a). Time-dependent MCF-7 cell death was also promoted by Res, regardless of caspase-3 expression (Figure 1b). The long-term consequences of Res treatment for cell survival are evident in colony-forming assay where the addition of Res resulted in a 37 and 58% reduction in the number of colonies of MCF-7^{casp-3} and MCF-7^{vc} cells, respectively (Figure 1c).

Moreover, Res induced a substantial arrest of the cell cycle in the S phase in both cell populations (Supplementary Figure S1). These data suggest that the effects of Res on cell proliferation and death are unrelated to caspase-3 expression.

Res does not induce caspase-dependent apoptosis when caspase-3 signaling is disrupted. To investigate the ability of Res to induce apoptosis, we performed a Hoechst 33258 (2′-(4-hydroxyphenyl)-5-(4-methyl-1-piperazinyl)-2,5′-bi-1*H*-benzimidazole trihydrochloride hydrate bis-benzimide) staining assay. Following Res treatment, MCF-7^{casp-3} cells displayed cellular changes (shrinkage, rounding, detachment, membrane blebbing and segregation of cellular structures), whereas MCF-7^{vc} cells displayed only insignificant hallmarks of DNA damage (Figure 2a, top). After Res treatment, the percentages of fragmented and condensed nuclei of MCF-7^{casp-3} cells at each of the time points were considerably higher than those of MCF-7^{vc} cells (Figure 2a, bottom).

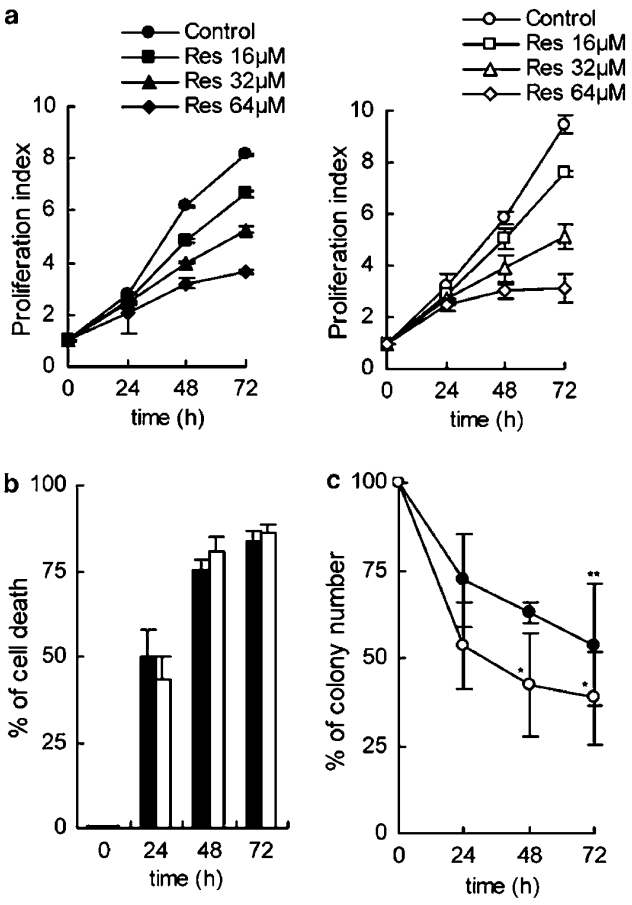

Figure 1 Res inhibits cell proliferation and promotes cell death. (**a**) Cell proliferation. The values correspond to mean ± S.D. of three independent experiments. (**b**) Cell death. Cells were treated with vehicle or 64 μM Res. Data were expressed as the percentage of dead cells relative to total cells. Data were normalized to vehicle-treated cells (taken to be 0%) and values were reported as mean ± S.D. of four independent experiments. (**c**) Colony formation. Cells were treated with vehicle or 64 μM Res and the number of colonies was measured *versus* vehicle-treated cells (taken to be 100%). The values were reported as mean ± S.D. of four independent experiments. Treatment with vehicle alone was the same as untreated cells. $^{**}P<0.01$; $^{*}P<0.05$ *versus* vehicle-treated cells. Full bars or symbols: MCF-7^{casp-3}; empty bars or symbols: MCF-7^{vc}

To find out whether the Res-induced appearance of apoptotic changes was correlated to the activation of caspase-3, we assessed the activity of caspase-3/7 enzyme and investigated the cleavage of poly(ADP-ribose) polymerase (PARP). After exposure to Res, we observed significant activation of caspase-3/7 (three-fold at 48 h and seven-fold at 72 h, *versus* the corresponding vehicle-treated cells) in MCF-7^{casp-3} cells (Figure 2b). The Res-induced activation of caspase-3 was corroborated by detection of an 85 kDa PARP fragment (Figure 2c). However, both caspase-3/7 activity and PARP cleavage were completely absent in Res-treated MCF-7^{vc} cells (Figure 2b and c).

These findings suggest that caspase-3 is required for the morphological and biochemical features of apoptosis observed after Res treatment.

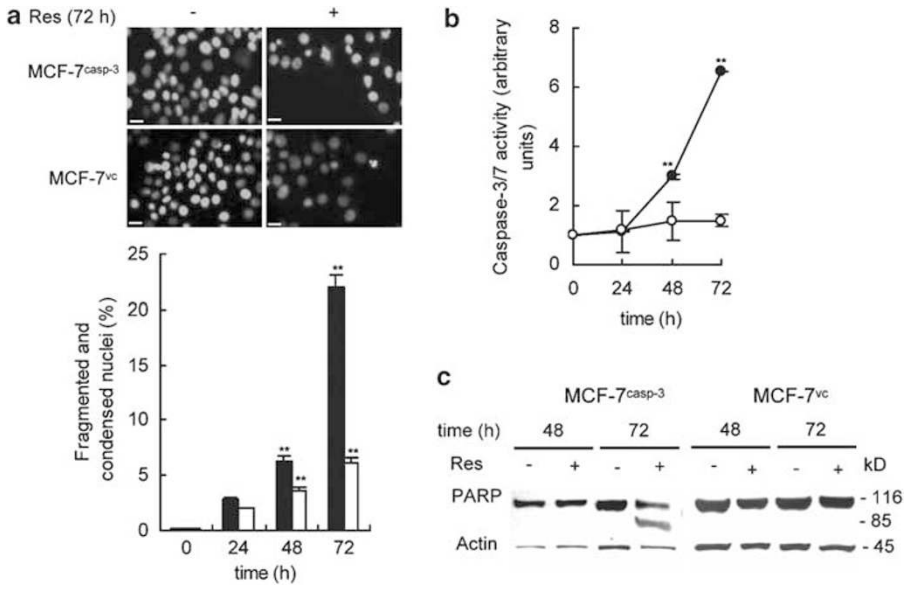

Figure 2 Res induces typical features of caspase-dependent apoptosis in MCF-7^{casp-3} cells. (**a**) Apoptosis morphology. Cells were treated with vehicle or 64 μM Res and a Hoechst staining was performed. (top) The picture shows one representative experiment out of five independent experiments. The bar corresponds to 1 μm. (bottom) Quantitative analysis of fragmented and condensed nuclei. Values were reported as mean ± S.D. of five independent experiments. The frequency of cells with fragmented and condensed nuclei was calculated relative to total cells. At least 100 cells were counted. (**b**) Caspase-3/7 activity. The level of enzymatic activity of caspase was normalized to total proteins in each sample. The results were expressed as arbitrary units per microgram protein (means ± S.D.) and represent the average of three data points. (**c**) PARP cleavage. Cells were treated with or without 64 μM Res. Protein levels of cleaved and uncleaved PARP and β-actin were detected by western blot. $^{**}P<0.01$ *versus* vehicle-treated cells. Full bars or symbols: MCF-7^{casp-3}; empty bars or symbols: MCF-7^{vc}

Res induces typical biomarkers of autophagy regardless of caspase-3 expression. To find out whether Res induced autophagy, we expressed GFP-LC3 in MCF-7^{casp-3} and MCF-7^{vc} cells. During autophagy, LC3 is relocated to the autophagosomal membranes. Thus, the accumulation of GFP-LC3 puncta provides an effective way of detecting autophagosomes.[16] The basal levels of autophagosomes were similar in MCF-7^{casp-3} and MCF-7^{vc} cells (Figure 3a). After Res treatment, both cell lines showed a significant increase in the number of cells with punctate fluorescence (Figure 3a, left). Indeed, after exposure to Res, the number of cells with punctate GFP-LC3 staining increased considerably, from 25 to 60% in MCF-7^{casp-3} cells, and from 27 to 84% in MCF-7^{vc} cells (Figure 3a, right).

We investigated the conversion of cytosolic LC3-I into LC3-II by western blotting. LC3-II levels correlate with the number of autophagosomes per cell.[16] Res elicited an increase in LC3-II of approximately 2.8- and 1.8-fold in MCF-7^{casp-3} and MCF-7^{vc} cells, respectively (Figure 3b, right). Because the cellular level of LC3-II alone may not accurately reflect autophagic activity,[17] the autophagic flux to the lysosomal compartment was investigated by analyzing LC3-II in cells pretreated with lysosomal cathepsin inhibitors (E64 ((2S,3S)-*trans*-epoxysuccinyl-L-leucylamido-3-methylbutane ethyl ester) and pepstatin A (Pep A)) and Res. After Res treatment, we observed an accumulation of LC3-II in the presence of lysosomal inhibitors (Figure 3b). Moreover, the rate of protein degradation was increased by Res in both cell populations (Figure 4a). As a positive control, we used C_2-ceramide (C_2-Cer), a typical autophagy promoter.[18] In both cell populations, C_2-Cer increased the percentage of GFP-LC3 punctate cells (Figure 3a) as well as autophagic flux (Figure 3c), and rate of proteolysis (Figure 4b). Taken together, these experiments show that both MCF-7^{casp-3} and MCF-7^{vc} cells are responsive to stimulation of autophagy by C_2-Cer and Res.

Even though autophagy was stimulated, the levels of typical autophagic proteins Atg7, Beclin 1 and hVps34 (or class III phosphoinositide 3-kinase (PI3K), which interacts with Beclin 1) were unchanged in both cell lines in response to Res (Supplementary Figure S2) in contrast to the level of LC3-II (Supplementary Figure S2). Furthermore, in both MCF-7^{casp-3} and MCF-7^{vc} cells, Res-induced autophagy was associated with inhibition of Akt/protein kinase B (PKB) phosphorylation and of mTOR signaling pathway as determined by the phosphorylation of S6K, a direct mTOR substrate (Figure 5a). These findings suggest that Res-induced autophagy is dependent on the inhibition of mTOR whatever the level of caspase-3 expression. According to our previous results,[18] C_2-Cer-induced autophagy is characterized by the inhibition of the Akt/PKB/mTOR signal in both MCF-7^{casp-3} and MCF-7^{vc} cells (Figure 5b).

Impairment of Atg-7-mediated autophagy reduces Res-induced cell death in MCF-7^{vc} cells. To investigate whether the inhibition of autophagy rescued MCF-7^{vc} cells from Res-induced cell death, we invalidated the expression of autophagic genes *ATG7* (autophagy-related gene), *BECN1* and *hVP34* (Figure 6a), and quantified autophagic vacuoles after transfection with GFP-LC3 plasmid. The presence of *ATG7*, *BECN1* and *hVPS34* siRNAs significantly reduced the basal GFP-LC3 puncta (Figure 6b, top) and the LC3-II levels (Figure 6b, middle and bottom). Treatment with both *ATG7* siRNA and Res reduced the

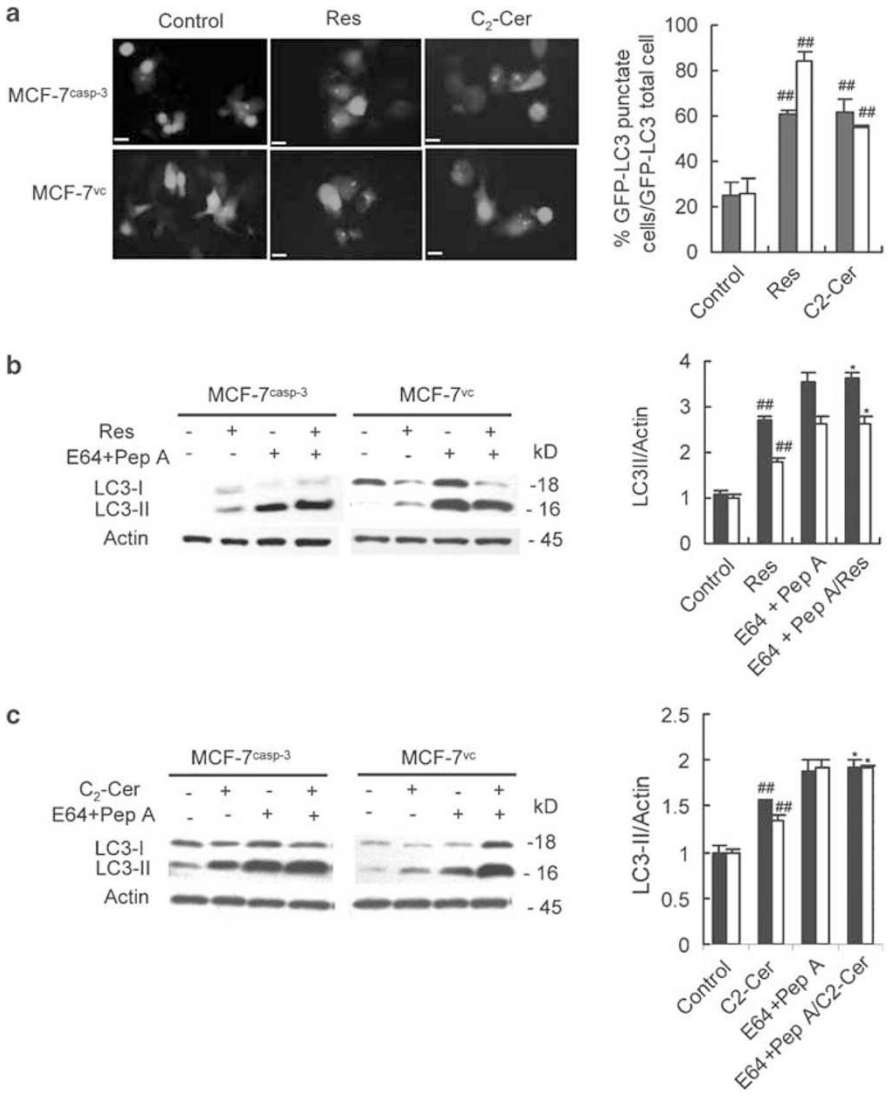

Figure 3 Res induces autophagy independently of caspase-3 expression. (**a**) Autophagosome formation. Cells were treated with vehicle (control), Res (64 μM, 48 h) or the positive control C_2-Cer (75 μM, 2 h) and then transfected with GFP-LC3 plasmid and examined by fluorescence microscopy. (left) The picture shows one representative experiment out of three independent experiments. The bar corresponds to 10 μm. (right) Quantitative analysis of GFP-LC3 cells. The percentage of GFP-positive cells with GFP-LC3 puncta was calculated. The results were expressed as mean ± S.D. from at least three independent experiments. (**b**, **c**) Autophagic flux. Cells were pretreated with lysosomal protease inhibitors, E64 + Pep A 10 μg/ml, and then with vehicle (control), Res (64 μM, 48 h) or C_2-Cer (75 μM, 2 h). Levels of the LC3-II and β-actin proteins were analyzed by western blot. Each picture shows one representative experiment out of five independent experiments. The ratio of LC3-II to actin levels in each experiment was determined densitometrically and normalized to vehicle values (taken to be 1). The values were expressed as the mean ± S.D. of five independent experiments. $^{\#\#}P<0.01$ *versus* vehicle-treated cells; $^{*}P<0.05$ *versus* Res- or C_2-Cer-treated cells. Solid bars: MCF-7^{casp-3}; empty bars: MCF-7^{vc}

number of cells with GFP-LC3 puncta compared to Res treatment. In contrast, the increase in autophagosome formation observed after Res exposure was not suppressed by the addition of *BECN1* or *hVPS34* siRNAs (Figure 6b, top). We observed a significant decrease in LC3-II after treatment with Res and *ATG7* siRNA, but not after Res and *BECN1* siRNA or *hVPS34* siRNA (Figure 6b, middle and bottom). As expected, blocking the expression of *ATG7*, *BECN1* or *hVPS34* genes significantly suppressed the GFP-LC3 puncta induced by C_2-Cer (Figure 6b, top). The autophagic inhibitor 3-MA was not able to prevent either the formation of GFP puncta (Supplementary Figure S3a) or the degradation of long-lived protein (Figure 4a) elicited by Res in MCF-7^{vc} cells. In contrast, C_2-Cer-induced proteolysis was counteracted by adding 3-MA (Figure 4b).

Next, to demonstrate that Res-induced cell death in MCF-7^{vc} cells was preferentially mediated by autophagy, we disabled autophagy and investigated cell death. The abrogation of *ATG7* gene expression consistently reduced cell death triggered by Res (Figure 6c, top). Conversely, disabling *BECN1* or *hVPS34* gene expression (Figure 6c, top) or adding 3-MA (Supplementary Figure S3b) did not inhibit Res-induced cell death. Moreover, Res-induced cell death was not reversed by adding z-VAD (*N*-benzyloxycarbonyl-Val-Ala-DL-Asp-fluoromethylketone; Figure 6c, bottom), and the effect of Res on the cell cycle was not mitigated after

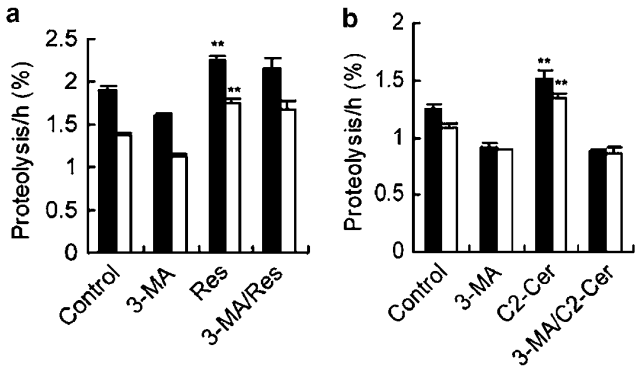

Figure 4 Res induces Beclin 1-independent autophagy. Degradation of long-lived proteins was determined in MCF-7 cells treated with vehicle (control) or 64 μM Res for 16 h (**a**) or 75 μM C_2-Cer for 2 h (**b**) in the presence or absence of 10 mM 3-MA. Values were reported as mean ± S.D. of three independent experiments. $^{**}P<0.01$ *versus* vehicle-treated cells. Solid bars: MCF-7^{casp-3}; empty bars: MCF-7^{vc}

treatment with *ATG7* or *BECN1* siRNAs (Supplementary Figure S1).

Res promotes necrotic death that is accentuated in MCF-7^{casp-3} cells. To investigate whether Res triggered additional caspase-independent cell death, we evaluated the occurrence of necrotic death by early membrane rupture. In response to Res, both MCF-7^{casp-3} and MCF-7^{vc} cells displayed biological aspects of necrosis, namely early plasma membrane rupture and cell dilatation (Figure 7a, left).

MCF-7^{casp-3} cells exhibited a significant increase in necrotic death within the first 24 h of incubation with Res (Figure 7a, right). The ability of Res to induce death with necrotic aspects was more evident in MCF-7^{casp-3} cells than in MCF-7^{vc} cells (Figure 7a). As a positive control, we use shikonin, a naturally occurring naphthoquinone, which is known to induce necrotic cell death in MCF-7 cells.[19] Shikonin induced cellular swelling in both cell populations (Figure 7b, left), but MCF-7^{casp-3} cells were more sensitive than MCF-7^{vc} cells (Figure 7b, right). Interestingly, in Res-treated MCF-7^{casp-3} cells, necrotic cell death was unaffected by adding z-VAD (data not shown).

To find out whether the increase in cell size produced by Res was due to induction of autophagy, we inhibited the gene expression of *ATG7*, *BECN1* or *hVPS34* and quantified necrotic cells. We confirmed that stimulation of autophagy was not involved in Res-induced necrosis and cell dilatation (Figure 7c, left). Accordingly, no change in cell volume was observed in C_2-Cer-treated cells before or after *BECN1* knockdown (Figure 7c, right). Our findings demonstrate that Res triggers several different types of cell death in MCF-7 cells, including necrosis.

Apoptosis rather than autophagy was responsible for cell death induced by Res in MCF-7^{casp-3} cells. To find out whether Res-induced cell death in MCF-7^{casp-3} was executed primarily through activation of caspase-dependent apoptosis, we pharmacologically inhibited the caspase-dependent pathways and evaluated the biological effects promoted by Res. The z-VAD treatment partially rescued cells from Res-induced death (Figure 8a, left) and partially

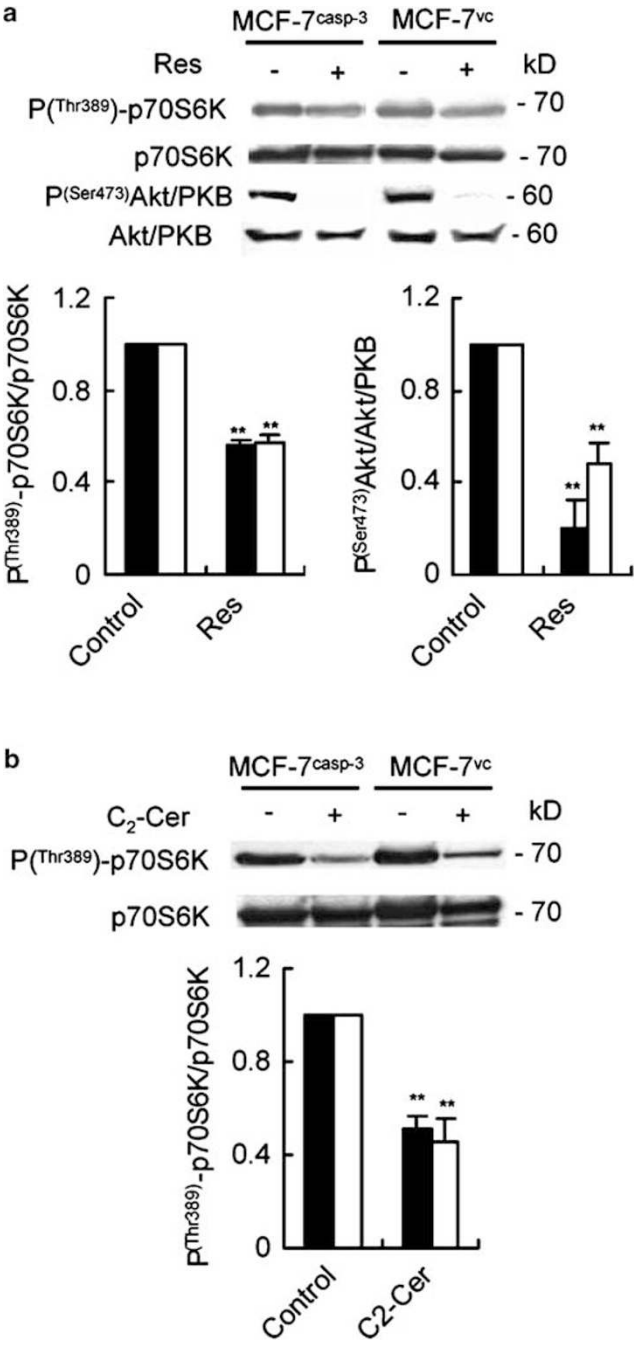

Figure 5 Res inhibits Akt/PKB phosphorylation and mTOR activity. (**a**) Protein levels of P(^{Ser473})Akt/PKB, Akt/PKB, P(^{Thr389})-p70S6K or p70S6K were analyzed by western blot after treatment with vehicle (control) or 64 μM Res for 48 h. Each picture shows one representative experiment out of three independent experiments. The ratio of P(^{Ser473})Akt/PKB to Akt/PKB and P(^{Thr389})-p70S6K to p70S6K level in each experiment was determined densitometrically and normalized to vehicle values (taken to be 1). (**b**) Protein levels of P(^{Thr389})-p70S6K or p70S6K were analyzed by western blot after treatment with vehicle (control) or 75 μM C_2-Cer for 2 h. The ratio of P(^{Thr389})-p70S6K to p70S6K level in each experiment was determined densitometrically and normalized to vehicle values (taken to be 1). $^{**}P<0.01$ *versus* vehicle-treated cells. Solid bars: MCF-7^{casp-3}; empty bars: MCF-7^{vc}

blocked the accumulation of apoptotic nuclei (Figure 8a, middle), but totally inhibited the generation of PARP

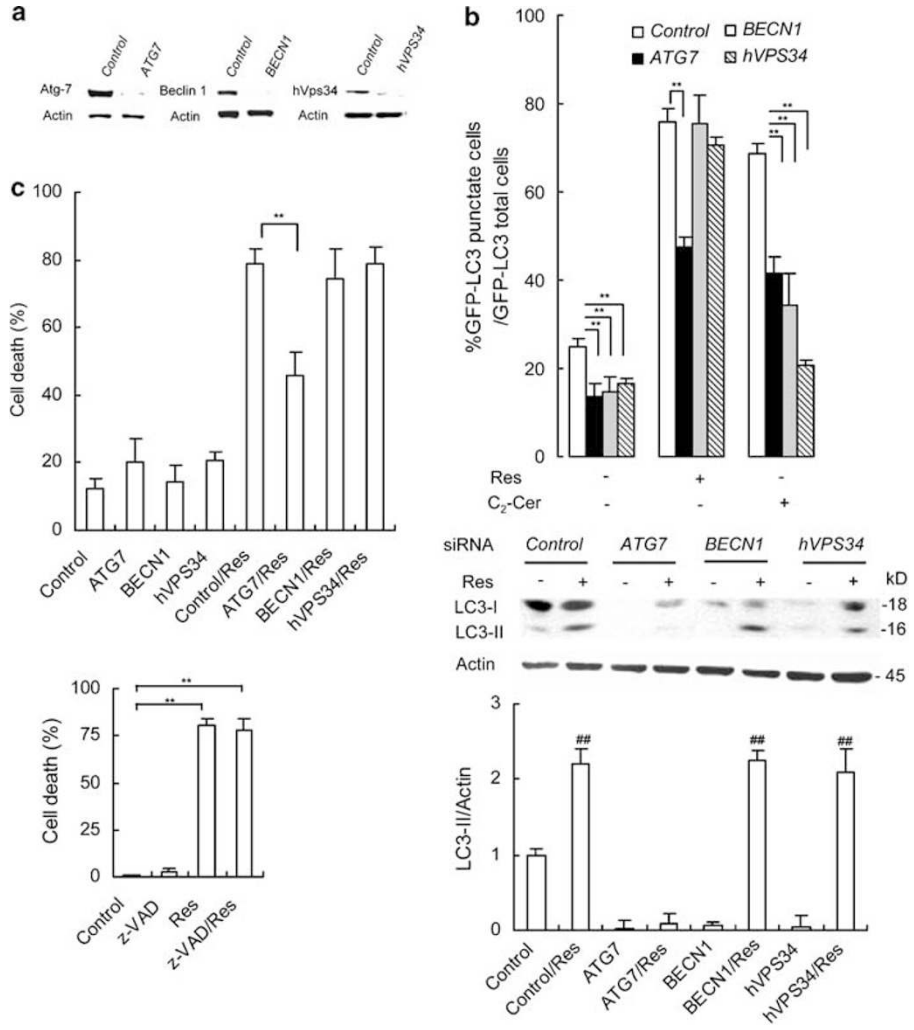

Figure 6 Cell death induced by Res is not only due to abrogation of autophagy gene expression in MCF-7^{vc} cells. (**a**) Effect of siRNAs on autophagy gene expression. Cells were transfected with control, *ATG7, BECN1* or *hVPS34* siRNAs for 72 h. The protein expression of Atg-7, Beclin 1 or hVps34 was monitored by western blot relative to β-actin. (**b**) Autophagic activity. (top) Cells were treated with vehicle, Res (64 μM, 48 h) or C_2-Cer (75 μM, 2 h) after transfection with control, *ATG7*, *BECN1* or *hVPS34* siRNAs. Quantification of autophagic vacuoles by fluorescence microscopy was performed after transfection with GFP-LC3 plasmid. The percentage of cells with GFP-LC3 puncta was calculated relative to total GFP-positive cells. The results were reported as mean ± S.D. from at least four independent experiments. (middle and bottom) Cells were treated with vehicle or 64 μM Res for 48 h after transfection with control, *ATG7*, *BECN1* or *hVPS34* siRNAs. Protein levels of LC3-II and β-actin were analyzed by western blot. Each picture shows one representative experiment out of three independent experiments. The ratio of LC3-II to actin levels in each experiment was determined densitometrically and normalized to vehicle values (taken to be 1). (**c**) Cell death. (top) Cells were incubated with control, *ATG7*, *BECN1* or *hVPS34* siRNAs for 24 h and then treated with vehicle or 64 μM Res for 48 h. (bottom) Cells were incubated with vehicle (control) or 64 μM Res in the presence or absence of 100 μM z-VAD for 48 h. Data were expressed as the percentage of dead cells relative to total cells. Data were normalized to vehicle-treated cells (taken to be 0%) and values were reported as mean ± S.D. of five independent experiments. $^{**}P<0.01$; $^{\#\#}P<0.01$ *versus control*-treated cells

fragments elicited by Res (Figure 8a, right). These findings suggest that Res triggers MCF-7^{casp-3} cell death by both caspase-dependent and caspase-independent mechanisms.

The suppression of *ATG7*, *BECN1* or *hVPS34* genes (Figure 8b) significantly reduced the accumulation of punctate GFP-LC3 (Figure 8c, top) and decreased the levels of LC3-II (Figure 8c, middle and bottom) in MCF-7^{casp-3} cells. Furthermore, Res-induced vacuolization and LC3-II levels were completely abolished only by *ATG7* siRNA and not by *BECN1* siRNA or *hVPS34* siRNA (Figure 8c, top and bottom). As expected, impairing the expression of autophagic genes consistently blocked the accumulation of punctate GFP-LC3 induced by C_2-Cer (Figure 8c, top).

As observed in MFC-7^{vc} cells, 3-MA was not able to reverse the formation of GFP-LC3 puncta (Supplementary Figure S3a), degradation of proteins (Figure 4a) or cell death (Supplementary Figure S3b) elicited by Res in MCF-7^{casp-3} cells. In contrast, the C_2-Cer-induced proteolysis was reversed after adding 3-MA (Figure 4b). These findings demonstrate that Res stimulates non-canonical Beclin 1-independent autophagy in MCF-7^{casp-3} cells.

Interestingly, the caspase inhibitor z-VAD did not suppress the accumulation of autophagic vacuoles observed after Res treatment (as assessed from the level of LC3-II) (Figure 8d, top and bottom) and GFP-LC3 staining (data not shown).

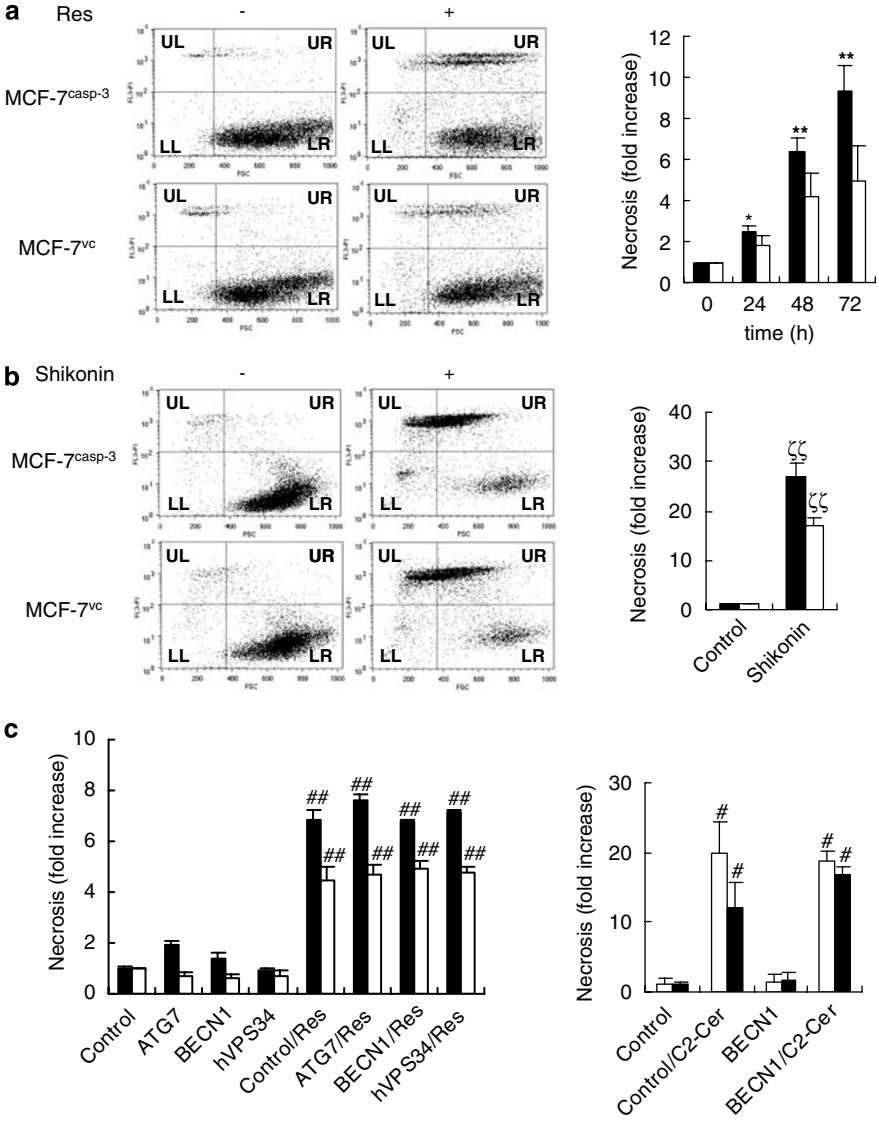

Figure 7 Res induces typical morphological features of necrotic cell death. (**a**) Necrotic cell death. (left) Graphs show cell size on the *X*-axis *versus* PI fluorescence on the *Y*-axis in cells after treatment with 64 μM Res for 72 h. Quadrants represent the distribution of small necrotic cells (UL), necrotic cells (UR), small cells with an intact membrane (LL) and live cells in 10 000 events. The picture shows one representative experiment out of six independent experiments. (right) The percentage of necrotic cells (UR) was normalized relative to vehicle-treated cells(taken to be 1). The results were expressed as the fold increase (mean ± S.D.) and represent the average of six independent experiments. (**b**) (left) Graphs show cell size on the *X*-axis *versus* PI fluorescence on the *Y*-axis in cells after treatment with vehicle (control) or 5 μM shikonin for 24 h. The picture shows one representative experiment out of three independent experiments. (right) The percentage of necrotic cells (UR) was normalized relative to vehicle-treated cells (taken to be 1). The results were expressed as the fold increase (mean ± S.D.) and represent the average of three independent experiments. (**c**) (left) Cells were transfected with control, *ATG7*, *BECN1* or *hVPS34* siRNAs for 24 h and then treated with vehicle or Res (64 μM, 48 h). At the end of treatment, necrosis was analyzed. (right) Cells were treated with vehicle or C_2-Cer (75 μM, 2 h) after 72 h of transfection with control or *BECN1 si*RNA and necrosis was analyzed. The percentage of necrotic cells (UR) was normalized relative to control-treated cells (taken to be 1). The results were expressed as the fold increase (mean ± S.D.) and correspond to the average of three independent experiments. $^{*}P<0.05$; $^{**}P<0.01$ MCF-7$^{casp\text{-}3}$ *versus* MCF-7^{vc}; $^{\zeta\zeta}P<0.01$ *versus* vehicle-treated cells; $^{\#}P<0.05$; $^{\#\#}P<0.01$ *versus* control-treated cells. Solid bars: MCF-7$^{casp\text{-}3}$; empty bars: MCF-7^{vc}

These findings support the hypothesis that autophagic vacuoles are formed further upstream and independently of the caspase-dependent death mechanism.

To clarify the caspase-independent cell death, we determined the effect of autophagic impairment on the ability of Res to execute cell death in the presence or absence of z-VAD. The abrogation of *ATG7*, *BECN1* or *hVPS34* gene expression did not affect cell death rescue obtained with z-VAD after Res treatment (Figure 8e). Incubation with the specific inhibitor of caspase-3, z-DEVD, leads to the same biological effects as those produced by z-VAD in MCF-7$^{casp\text{-}3}$ cells (data not shown). Moreover, knockdown of *ATG7* did not modify the percentage of Res-induced cell death (Figure 8e), nor prevented the appearance of an apoptotic morphology (data not shown). In addition, the Res-induced accumulation of cells in the S phase was not modified after knocking down *ATG7* or *BECN1* (Supplementary Figure S1).

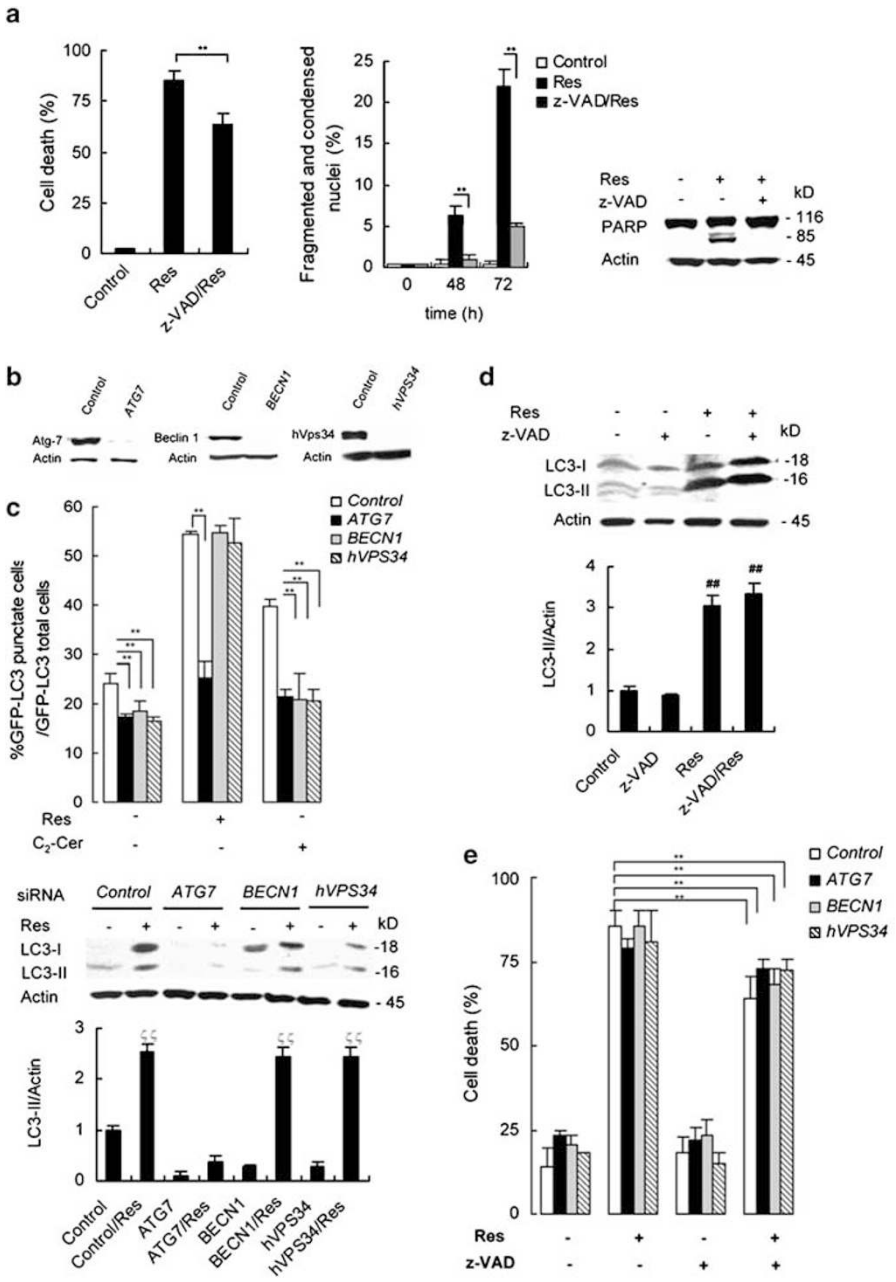

Figure 8 Res triggers MCF-7^{casp-3} cell death by both caspase-dependent and caspase-independent mechanisms. (**a**) Caspase-dependent apoptotic death. Cells were incubated with vehicle (control) or 64 μM Res in the presence or absence of 100 μM z-VAD and cell death (left), nuclear DNA morphology (middle) and PARP cleavage (right) were tested. Cell death was measured after 72 h treatment and data were expressed as the percentage of dead cells. Data were normalized to vehicle-treated cells (taken to be 0%) and values were reported as mean ± S.D. of three independent experiments. The Hoechst DNA staining was assessed by fluorescent microscopy and values were expressed as mean ± S.D. of three independent experiments. Protein levels of cleaved PARP and β-actin were detected by western blotting after 72 h of treatment. Treatment with z-VAD alone was the same as that of vehicle-treated cells. (**b**) Effect of siRNAs on autophagic gene expression. Cells were transfected with control, *ATG7*, *BECN1* or *hVPS34* siRNAs for 72 h. The Atg-7, Beclin 1 and hVps34 protein expressions were monitored by western blot relative to β-actin. (**c**) Autophagic activity. (top) Cells were treated with vehicle or Res (64 μM, 48 h) or C_2-Cer (75 μM, 2 h) after transfection with control, *ATG7*, *BECN1* or *hVPS34* siRNAs. Quantification of autophagic vacuoles by fluorescence microscopy was performed after transfection with the GFP-LC3 plasmid. The percentage of cells with GFP-LC3 puncta was calculated relative to total GFP-positive cells. The results were reported as mean ± S.D. from at least four independent experiments. (middle and bottom) Cells were treated with vehicle or 64 μM Res for 48 h after transfection with control, *ATG7*, *BECN1* or *hVPS34* siRNAs. Protein levels of LC3-II and β-actin were analyzed by western blot. Each picture shows one representative experiment out of three independent experiments. The ratio of LC3-II to actin levels in each experiment was determined densitometrically and normalized to vehicle values (taken to be 1). (**d**) Evaluation of LC3-II. Cells were treated with vehicle (control) or 64 μM Res in the presence or absence of 100 μM z-VAD. Protein levels of LC3-II and β-actin were analyzed by western blot. Each picture shows one representative experiment out of three independent experiments. The ratio of LC3-II to actin levels in each experiment was determined densitometrically and normalized to vehicle values (taken to be 1). (**e**) Cell death. Cells were incubated with control, *ATG7*, *BECN1* or *hVPS34* siRNAs for 24 h and then treated with 64 μM Res in the presence or absence of 100 μM z-VAD. Data were expressed as the percentage of dead cells relative to total cells. Data were normalized to vehicle-treated cells (taken to be 0%) and values were reported as mean ± S.D. of six independent experiments. $^{**}P<0.01$; $^{\text{ςς}}P<0.01$ *versus* control-treated cells; $^{\#\#}P<0.01$ *versus* vehicle-treated cells

These findings demonstrate that in MCF-7^{casp-3} cells, the Res-induced Beclin 1-independent autophagy is unrelated to cell death.

Additionally, to verify that the dissimilarity in autophagy inhibition between Res and C_2-Cer treatment was not due to differences in timing or to induction of cell death by Res, we tested LC3-II levels after different treatment times. In both cell populations, exposure to Res for a short time (16 h, when cell death is barely detectable) increased the autophagic flux as determined by the analysis of the rate of protein degradation (Figure 4a) and LC3-II level in the presence of lysosomal inhibitors (Supplementary Figure S4).

To confirm that the role of Beclin 1-independent autophagy in cell death is unrelated to inhibition of caspase-3, we tested Res in caspase-3-positive MDA-MB-231, a highly invasive and metastatic breast cancer cell line. The silencing of *ATG7* or *BECN1* gene expression (Supplementary Figure S5a) significantly reduced the accumulation of GFP-LC3 puncta (Supplementary Figure S5b) in MDA-MB-231 cells. However, we found that cell death was not totally blocked after z-VAD treatment (Supplementary Figure S5c) similar to inhibition of fragmented and condensed nuclei induced by Res (Supplementary Figure S5d). By silencing of autophagic gene expression, we observed that Res-induced GFP-LC3 puncta were independent of Beclin 1, but dependent on Atg7 (Supplementary Figure S5b). However, knockdown of *ATG7* did not modify the percentage cell death observed in the presence or absence of z-VAD (Supplementary Figure S5c).

These data support the conclusion that Res induces both caspase-dependent and caspase-independent cell death in MCF-7^{casp-3} cells concomitantly to activating Beclin 1-independent autophagy. The role of Beclin 1-independent autophagy in cell death is therefore not dependent on inhibition of caspase-3.

To investigate whether the expression of caspase-3 governs the role of non-canonical autophagy in Res-induced cell death, we knocked down *CASP3* gene in MCF-7^{casp-3} cells (Figure 9a). As shown in Figure 9b, the *CASP3* gene silencing protected cells against Res-induced cell death after depletion of *ATG7* gene, but not after depletion of *BECN1* gene. To confirm the relationship between the expression of caspase-3 and the role of non-canonical autophagy in Res-induced cell death, we transfected MCF-7^{vc} cells with cDNA encoding the wild-type caspase-3 (casp-3WT) and cDNA encoding a mutant inactive form of caspase-3 (casp-3C163S) (Figure 9d). We observed that knockdown of *ATG7* was no longer able to rescue cells expressing the casp-3C163S mutant from Res-induced cell death (Figure 9c and e). From these results, we demonstrated that the caspase-3 protein but not its activity is enough to block Beclin 1-independent autophagic cell death in MCF-7 cells.

Discussion

Caspase-3 is the major downstream effector of caspase-dependent cell death, and is usually activated by various death signals and cleaves important cellular proteins.[20,21]

Many malignant cells, such as MCF-7 human breast cells, have lost the ability to undergo normal apoptosis,[22] caspase-3 is necessary for apoptosis-related nuclear events[12,23] but it

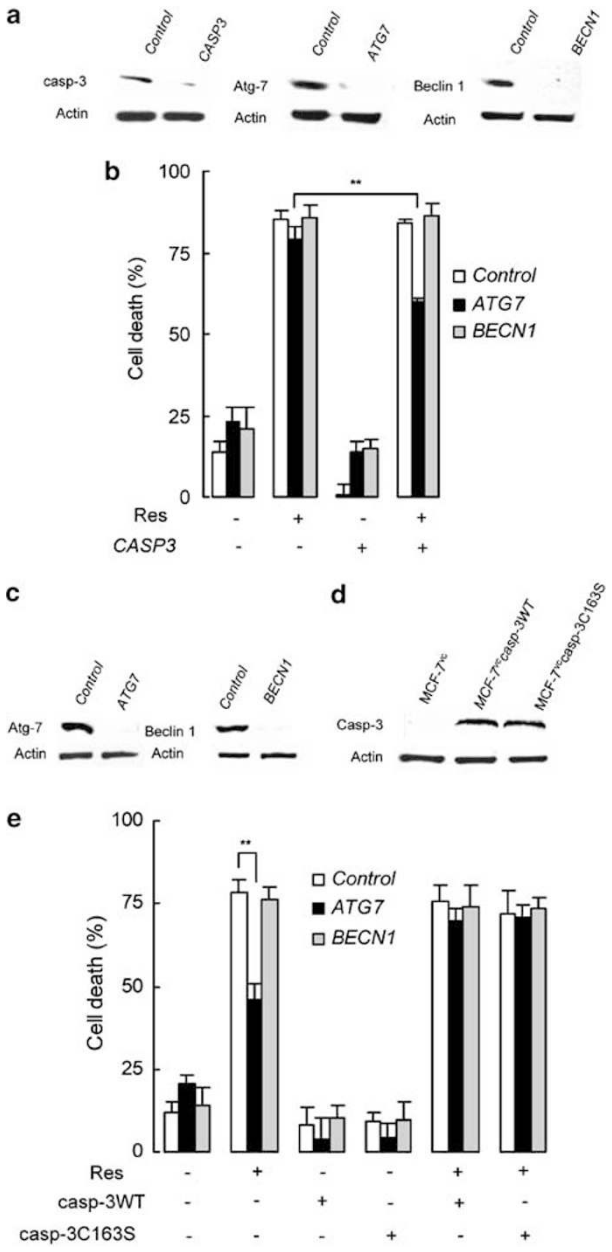

Figure 9 The caspase-3 protein blocks autophagic cell death in MCF-7 cells independently of its catalytic activity. (**a**) Effect of siRNAs on the expression of caspase-3 and of autophagic genes in MCF-7^{casp-3} cells. Cells were transfected with control, *CASP3*, *ATG7* or *BECN1* siRNAs for 72 h. The caspase-3, Atg-7 and Beclin 1 protein expressions were monitored by western blot relative to β-actin. (**b**) Cell death. MCF-7^{casp-3} cells were incubated with control, *CASP3*, *ATG7* or *BECN1* siRNAs for 24 h and then treated with 64 μM Res for 48 h. Data were expressed as the percentage of dead cells relative to total cells. Data were normalized to vehicle-treated cells (taken to be 0%) and values were reported as mean ± S.D. of three independent experiments. (**c**) MCF-7^{vc} cells were transfected with control, *ATG7* or *BECN1* siRNAs for 72 h. Atg-7 and Beclin 1 protein expressions were monitored by western blot relative to β-actin. (**d**) The protein expression of caspase-3 in MCF-7^{vc}, MCF-7^{vc}casp-3WT and MCF-7^{vc}casp-3C163S cells was assessed by western blot relative to β-actin. (**e**) Cell death. MCF-7^{vc} cells were incubated with control, *ATG7* or *BECN1* siRNAs for 24 h and then with 1.0 μg of casp-3WT or casp-3C163S plasmids in the presence or absence of 64 μM Res for 48 h. Data were expressed as the percentage of dead cells relative to total cells. Data were normalized to vehicle-treated cells (taken to be 0%) and values were reported as mean ± S.D. of three independent experiments. $^{**}P < 0.01$

may not be important for cell death, and a deficit in caspase-3 is not sufficient to block Bax-induced cell death in MCF-7 cells.[24]

The purpose of this study is to explore the hypothesis that Res uses autophagy to kill those cells that are unresponsive to drugs that target caspase-dependent apoptotic cell death.

We found that Res exerts a robust antiproliferative effect, induces mortality and reduces the number of colonies in a time-dependent manner in both cell populations. Nevertheless, MCF-7^{vc} cells are more sensitive to cell death and growth inhibition elicited by Res. These findings are consistent with those showing that disabled apoptosis results in increased radiosensitivity in MCF-7 cells,[25] Bax/Bak$^{-/-}$ double knockout embryonic fibroblasts[26] and the PC3 prostate cell line.[27] Autophagy contributes to cell death in connection with the inhibition of apoptosis, improving tumor cell killing.[28] Moreover, in our study, Res induced a substantial arrest of the cell cycle in the S phase. This ability was most probably due to inhibition of ribonucleotide reductase.[29]

Following Res treatment, only the apoptotic-competent MCF-7 cells display the characteristic morphological signs of apoptosis. Thus, when the caspase machinery is active, Res induces cell death by activating caspase-dependent pathways. We assume that genetic constitution and activated signal pathways present in a cancer cell might determine how death is triggered after the chemotherapeutic stimulus. In MCF-7$^{casp\text{-}3}$ cells, Res triggers both caspase-dependent and caspase-independent cell death, bearing the characteristic hallmarks of necrosis. The ability of Res to elicit necrotic cell death has already been reported in DU145 prostate cells.[30]

Res stimulates both apoptosis and autophagy in ovarian carcinoma cells.[8] Here, we found that in MCF-7 cells, Res increases both GFP-LC3 puncta and LC3-II levels via the Atg7 protein.

Nevertheless, our data indicate that the regulation of autophagy activated by Res differs from that of C_2-Cer-induced autophagy. We found that the autophagic process induced by Res is completely independent of hVps34. Zhu *et al*.[31] were the first to show the existence of an hVps34/Beclin 1-independent mechanism of autophagy elicited by neurotoxin 1-methyl-4-phenylpyridinium in pathological situations. Recently, it has been observed that 3-MA did not block autophagy or genesis of vacuoles in miniprotoplasts.[32] Interestingly, in A2780 ovarian cancer cells, which have high levels of Bcl-2/Bcl-x_L, which inhibits Beclin 1-dependent autophagy,[33] the effect of Res on autophagy is not invalidated.[8] Overall, this finding supports the existence of a new type of autophagy that is insensitive to PI3K inhibitors.

Nevertheless, further investigations are needed to elucidate the molecular mechanism by which hVps34/Beclin 1-independent autophagy is regulated upstream of the Atg12 and LC3 conjugation systems. However, both canonical (induced by C_2-Cer) and non-canonical (induced by Res) autophagies are characterized by the inhibition of mTOR signaling. mTOR acts upstream of the Atg1 complex,[34] which suggests that autophagy induced by either Res or C_2-Cer uses this pathway to trigger the formation of autophagosomes.

When the non-canonical autophagy is invalidated in MCF-7$^{casp\text{-}3}$ cells, the caspase-independent cell death triggered by Res is neither attenuated nor enhanced. Moreover, in this cell line, the non-canonical autophagy is unconnected to the caspase-activation signal. The accumulation of autophagic vacuoles seems to occur upstream of apoptotic cell death. However, blocking caspase activity in both MCF-7$^{casp\text{-}3}$ and MDA-MB-231 cells does not uncover a cell death activity for Res-dependent non-canonical autophagy. This contrasts with other settings, where canonical autophagy has been shown to be used as a backup cell death mechanism after caspase inhibition.[35]

In this study, we show that the expression of caspase-3, but not its enzymatic activity, is able to modulate the role of non-canonical autophagy in Res-induced cell death after depletion of *ATG7*. It has been shown that the expression of caspase-3 inhibits growth of MCF-7 cells independently of its catalytic activity,[36] indicating that caspase-3 expression could activate regulatory intracellular pathway(s) other than apoptosis, for example, phosphorylation of AKT. On the basis of these findings, we deduce that this non-canonical form of autophagic cell death is blocked by the expression of caspase-3, but not by its enzymatic activity.

In neurons, Beclin 1-independent autophagy triggered cell death in response to the neurotoxin 1-methyl-4-phenylpyridinium occurs in the absence of caspase activation.[31] A better understanding of the role of non-canonical autophagy calls for an understanding of its molecular control, that is, its regulation and the molecular machinery required to form autophagosomes.

Many targets for Res have been identified *in vitro*,[7] such as the NAD^+-dependent deacetylase Sir2/SIRT1.[37] Stimulation of the class I PI3K/PKB signaling pathway by growth factors and cytokines has an inhibitory effect on autophagy in many cell types, and in mammalian cells AMP-activated protein kinase was required for autophagy.[38] Moreover, the inhibition of insulin-induced PI3K–PKB–Forkhead box O signaling cascade was due to a direct inhibitory effect of Res on class IA PI3K. It has recently been shown that Res inhibits Akt/PKB and mTOR activation, two downstream kinases of class I PI3K, in ovarian cancer cells.[39] In line with these findings, we now report that Res inhibits the activation of Akt/PKB and mTOR in breast cancer cells. These data suggest that the non-canonical autophagy is triggered by mTOR inhibition in a manner similar to canonical autophagy.

Despite the fact that the specific molecular players involved in non-canonical autophagy remain to be identified, our study shows that breast cancer cells can use the activation of this pathway as a cell death mechanism acting independently of the tumor suppressor Beclin 1.

Materials and Methods

Reagents. C_2-Cer dissolved in ethanol, 1,7-amino-4-trifluoromethyl coumarin, sulforhodamine B, Hoechst 33258, protease inhibitor mixture (PIC), Trypan blue, propidium iodide (PI), Pep A, E64 and 3-MA were from Sigma. Res dissolved in ethanol was from Cayman Chemical Company. Shikonin dissolved in DMSO was from Biomol International, LP. The caspase-3 colorimetric assay kit was from Calbiochem. z-VAD was from MBL International Corporation. RPMI 1640 medium, Dulbecco's modified Eagle's medium, fetal bovine serum and the LiteAblot® chemiluminescent substrate for western blot were from Euroclone. The Coomassie plus™ protein assay kit was purchased from Pierce. Nitrocellulose membranes were from Amersham. The rabbit polyclonal anti-Beclin 1, anti-P(^{Thr389})-p70S6K, anti-p70S6K, anti-P(^{Ser473})Akt, anti-Akt/PKB, anti-caspase-3 and anti-β-actin were from

Cell Signaling. The rabbit polyclonal anti-LC3 was from Novus Biologicals. Rabbit polyclonal anti-PARP was from Santa Cruz Biotechnology. The rabbit polyclonal anti-Atg7 was kindly provided by WA Dunn (University of Florida, Gainesville). The rabbit polyclonal anti-Vps34 was from Abgent Inc. Peroxidase-conjugated goat anti-rabbit IgG (H + L) was obtained from Jackson ImmunoResearch Laboratories Inc. All siRNAs for human proteins and silencer negative control (control siRNA) were synthesized by Ambion. Oligofectamine, Lipofectamine and Opti-MEM® I Reduced Serum Medium were from Invitrogen. pEGFP empty vector was from BD Biosciences.

Cell culture and transfection. Human breast cancer cells control vector MCF-7^{vc} and pcDNA3-casp-3-transfected MCF-7$^{casp\text{-}3}$ cells were the kind gifts of Dr. PT Daniel (Humboldt University, Berlin, Germany). MCF-7 cells were maintained at 37°C in 5% CO_2 in RPMI 1640, supplemented with 10% fetal bovine serum and 100 ng/ml each of penicillin and streptomycin. The human breast carcinoma cell line MDA-MB-231 from American Type Culture Collection was maintained at 37°C in 5% CO_2 in Dulbecco's modified Eagle's medium, supplemented with 5% fetal bovine serum and 100 ng/ml each of penicillin and streptomycin.

The plasmid expression vector encoding GFP-LC3 (pEGFP-LC3) was kindly provided by T Yoshimori (Research Institute for Microbial Diseases, Osaka University, Osaka, Japan).

siRNAs and treatments. siRNAs for human proteins were synthesized using the following target gene sequences: 5′-GGAGUCACAGCUCUUCCUU-3′ for *ATG7*, 5′-CAGUUUGGCACAAUCAAUA-3′ for *BECN1*, 5′-ACUCAACACUGGCU AAUUA-3′ for *hVPS34* and 5′-UGACAUCUCGGUCUGCUAC-3′ for *CASP3*. The control siRNA was composed of a 19-bp non-target sequence with 3′ dT overhangs. MCF-7 cells were seeded, and after 24 h transfected in Opti-MEM I Reduced Serum Medium with 50 nmol/l control siRNA, 50 nmol/l *BECN1* siRNA, 25 nmol/l *ATG7 si*RNA, 25 nmol/l *hVPS34* siRNA or 25 nmol/l *CASP3* siRNA for 4 h using Oligofectamine as recommended by the manufacturer. After 24 h of siRNA treatment, vehicle or Res was added for 48 h. C_2-Cer was added for 2 h after 72 h of siRNA treatment. At the end of the experiments, cells were collected and the level of protein expression was evaluated by western blotting.

Construction of human caspase-3 mutant. The human caspase-3 cDNA cloned into the pCMV6-XL5 (pCMV-Caspase-3) expression vector was purchased from Origene (Rockville, MD, USA). The pCMV-Caspase-3 plasmid vector was subjected to site-directed mutagenesis using the QuickChange Site-Directed Mutagenesis Kit (Stratagene, La Jolla, CA, USA) according to the manufacturer's instructions.

The Cys163Ser substitution was engineered with two mutagenic primers: primer A, 5′-CCCAAACTTTTCATTATTCAGGCCAGCCGTGGTACAGAAC-3′, and the reverse primer B, 5′-GTTCTGTACCACGGCTGGCCTGAATAATGAAAAGTTTGG G-3′. The mutated base is underlined. The construct was verified by sequencing.

Measurement of caspase-3/7 activity. Caspase-3/7 activity was determined using the caspase-3 colorimetric assay kit as described by the manufacturer. Briefly, after lysis, cell extracts were used to determine caspase-3/7 activity by adding the peptide substrate acetyl-Asp-Glu-Val-Asp *p*-nitroanilide (Ac-DEVD-pNA). In this assay, cleavage of the peptide by the caspase releases pNA, which has a high absorbance at 405 nm. The concentration of pNA released from the substrate was calculated from a calibration curve prepared using defined pNA solutions. The experiments were performed in triplicate.

Necrosis analysis. Necrosis was measured using PI exclusion as previously described. Briefly, 3×10^5 cells/well were seeded in six-well plates and allowed to adhere for 24 h. Cells were treated and at the end of the treatment, cells and medium were collected and cells were stained with PI (5 μg/ml) for 5–10 min. Stained cells were analyzed by flow cytometry (FACSorter, Becton Dickinson). Live gating of the forward and side scatter channels was used to exclude debris and to acquire cell events selectively. Individual fluorescence populations were determined using acquisition and quadrant analysis software (Cell Quest, Becton Dickinson). The experiments were performed in triplicate.

Cell cycle analysis. Cell cycle profile was analyzed by flow cytometric analysis by DNA staining with PI. After treatment, cells were collected, washed with phosphate-buffered saline (PBS) and fixed in 70% ethanol at −20°C. Cells were collected by centrifuging and resuspended in 1 ml PBS containing 50 μg/ml PI for 1 h at room temperature. Stained cells were analyzed by flow cytometry on the FACSorter (Becton Dickinson). The percentage of cells in different phases of the cell cycle was determined using the CellQuest software program.

Immunoblotting. Cells were collected by centrifuging (10 min, at 300 × *g*), washed with PBS and resuspended in lysis buffer (1% Triton X-100, 5 mM NaCl, 50 mM Tris-HCl pH 7.4, 10% glycerol, 1 mM phenylmethylsulfonyl fluoride, 1% PIC, 1 mM Na_3VO_4, 1 mM NaF) for 1 h on ice. The cell lysate was centrifuged (20 000 × *g* for 30 min at 4°C) and the supernatant was recovered. Protein concentrations were determined by Coomassie reagent as recommended by the manufacturer. Extracted proteins were first separated in sodium dodecyl sulfate-polyacrylamide gels and then electrotransferred onto nitrocellulose membranes. After blocking for 1 h with fat-free milk, the membranes were incubated with appropriate primary antibodies overnight: anti-Beclin 1 (1 : 10 00), anti-PARP (1 : 500), anti-Atg7 (1 : 4000), anti-hVps34 (1 : 1000), anti-LC3 (1 : 500), anti-P(^{Thr389})-p70S6K (1 : 1000), anti-p70S6K (1 : 1000), anti-P(^{Ser473})Akt (1 : 1000), anti-Akt/PKB (1 : 1000), anti-caspase-3 (1 : 1000) and anti-β-actin (1 : 1000). Primary antibodies were detected by chemiluminescence using horseradish peroxidase-conjugated secondary antibodies against rabbit immunoglobulin. Fluorographs were quantitatively scanned using the Quantity-One software (Bio-Rad).

Sulforhodamine B proliferation assay. Cells were seeded in 96-well tissue culture plates and allowed to adhere for 24 h before treatment. Cell proliferation was assessed at various time points during treatment with Res by sulforhodamine B monosodium salt assay. Five replicates were used for each treatment. Data are expressed as the proliferation index (fold increase of proliferation *versus* vehicle-treated cells at time zero).

Cell death. Cell death was determined by Trypan blue exclusion test as described previously.[18] Triplicate samples were used for each treatment. Dead cells were counted by Trypan blue exclusion assay.

Clonogenic assay. Cells were seeded in six-well tissue culture plates and allowed to adhere for 24 h before treatment. Triplicate samples were used for each treatment. The medium containing the treatment was replaced by drug-free medium after the indicated time points. As the colonies became visible (14 days), the cells were fixed with methanol, stained with Giemsa (1 : 10 in H_2O by volume) and counted.

GFP-LC3 staining. When required, the cells were treated for the times indicated and transfected with 1 μg of GFP-LC3 plasmid for 24 h in Opti-MEM I Reduced Serum Medium by Lipofectamine as recommended by the manufacturer. GFP-LC3 dot staining was visualized using an Axioplan Zeiss microscope and the number of GFP-positive cells with GFP-LC3 dots was determined. More than 100 transfected cells were counted by two investigators. Only cells with at least five dots were scored as positive. Duplicate samples were used for each treatment.

Proteolysis. The rate of long-lived protein degradation was measured as described previously.[40] Briefly, cells were incubated for 24 h at 37°C in normal culture medium containing 7400 Bq/ml of [^{14}C]valine. Cells were rinsed three times with PBS (pH 7.4) and then incubated in complete medium supplemented with 10 mM valine. After incubation for 1 h, the medium was replaced by fresh chase medium for an additional 4 h. When required, Res (64 μM, 16 h) or C_2-Cer (75 μM, 2 h) and 3-MA (10 mM) were added to the chase medium. Cells and radiolabeled proteins from the 4-h chase medium were precipitated in trichloroacetic acid at a final concentration of 10% (v/v) at 4 °C. Radioactivity was determined by liquid scintillation counting. Protein degradation was calculated by dividing the acid-soluble radioactivity recovered from both cells and medium by the radioactivity contained in the precipitated proteins from both cells and medium. Triplicate samples were used for each treatment.

Hoechst staining. Treated cells were fixed with 3.7% paraformaldehyde for 30 min and then stained with Hoechst 33258 (0.5 μg/ml) for 15 min at room temperature. One hundred cells were counted under an Axiovert fluorescence microscope and were scored according to the incidence of apoptotic chromatin changes. Duplicate samples were used for each treatment.

Statistical analysis. Statistical analysis of the differences between the groups was performed using Student's *t*-test. Significance was established when $P < 0.05$.

Acknowledgements. We thank T Yoshimori for providing us GFP-LC3, PT Daniel for sharing human transfectant MCF-7^{vc} and MCF-7^{casp-3} cells and William Dunn (University of Florida, Gainesville, FL, USA) for the Atg7 antibody. We are especially indebted to Riccarda Granata (University of Turin, Italy) for inestimable suggestions and critical reading of the manuscript. We wish to thank Dr. Iacopo Gesmundo (University of Turin) for excellent technical assistance with western blot. This study was supported by fellowships from FIRC (to Francesca Scarlatti) and University of Milan (to Roberta Maffei), by Institutional grants from University of Milan, INSERM and Université Paris Sud 11, and by research grants from the Association pour la Recherche sur le Cancer (no. 3503) in P Codogno's laboratory and from Fondazione Cariplo in R Ghidoni's laboratory.

Addendum

While this manuscript was being revised, sirtuin 1, the target of resveratrol, was shown to regulate macroautophagy (Lee *et al. Proc Natl Acad Sci* USA 2008; **105**: 3374–3379).

1. Klionsky DJ, Ohsumi Y. Vacuolar import of proteins and organelles from the cytoplasm. *Annu Rev Cell Dev Biol* 1999; **15**: 1–32.
2. Mizushima N. The pleiotropic role of autophagy: from protein metabolism to bactericide. *Cell Death Differ* 2005; **12** (Suppl 2): 1535–1541.
3. Klionsky DJ, Cregg JM, Dunn Jr WA, Emr SD, Sakai Y, Sandoval IV *et al.* A unified nomenclature for yeast autophagy-related genes. *Dev Cell* 2003; **5**: 539–545.
4. Clarke PG. Developmental cell death: morphological diversity and multiple mechanisms. *Anat Embryol (Berl)* 1990; **181**: 195–213.
5. Kondo Y, Kanzawa T, Sawaya R, Kondo S. The role of autophagy in cancer development and response to therapy. *Nat Rev Cancer* 2005; **5**: 726–734.
6. Scarlatti F, Sala G, Somenzi G, Signorelli P, Sacchi N, Ghidoni R. Resveratrol induces growth inhibition and apoptosis in metastatic breast cancer cells via *de novo* ceramide signaling. *FASEB J* 2003; **17**: 2339–2341.
7. Signorelli P, Ghidoni R. Resveratrol as an anticancer nutrient: molecular basis, open questions and promises. *J Nutr Biochem* 2005; **16**: 449–466.
8. Opipari Jr AW, Tan L, Boitano AE, Sorenson DR, Aurora A, Liu JR. Resveratrol-induced autophagocytosis in ovarian cancer cells. *Cancer Res* 2004; **64**: 696–703.
9. Tessitore L, Davit A, Sarotto I, Caderni G. Resveratrol depresses the growth of colorectal aberrant crypt foci by affecting bax and p21(CIP) expression. *Carcinogenesis* 2000; **21**: 1619–1622.
10. Carbo N, Costelli P, Baccino FM, Lopez-Soriano FJ, Argiles JM. Resveratrol, a natural product present in wine, decreases tumour growth in a rat tumour model. *Biochem Biophys Res Commun* 1999; **254**: 739–743.
11. Baur JA, Sinclair DA. Therapeutic potential of resveratrol: the *in vivo* evidence. *Nat Rev Drug Discov* 2006; **5**: 493–506.
12. Janicke RU, Sprengart ML, Wati MR, Porter AG. Caspase-3 is required for DNA fragmentation and morphological changes associated with apoptosis. *J Biol Chem* 1998; **273**: 9357–9360.
13. Pozo-Guisado E, Merino JM, Mulero-Navarro S, Lorenzo-Benayas MJ, Centeno F, Alvarez-Barrientos A *et al.* Resveratrol-induced apoptosis in MCF-7 human breast cancer cells involves a caspase-independent mechanism with downregulation of Bcl-2 and NF-kappaB. *Int J Cancer* 2005; **115**: 74–84.
14. Kim YA, Choi BT, Lee YT, Park DI, Rhee SH, Park KY *et al.* Resveratrol inhibits cell proliferation and induces apoptosis of human breast carcinoma MCF-7 cells. *Oncol Rep* 2004; **11**: 441–446..
15. Li Y, Liu J, Liu X, Xing K, Wang Y, Li F *et al.* Resveratrol-induced cell inhibition of growth and apoptosis in MCF7 human breast cancer cells are associated with modulation of phosphorylated Akt and caspase-9. *Appl Biochem Biotechnol* 2006; **135**: 181–192.
16. Kabeya Y, Mizushima N, Ueno T, Yamamoto A, Kirisako T, Noda T *et al.* LC3, a mammalian homologue of yeast Apg8p, is localized in autophagosome membranes after processing. *EMBO J* 2000; **19**: 5720–5728.
17. Tanida I, Minematsu-Ikeguchi N, Ueno T, Kominami E. Lysosomal turnover, but not a cellular level, of endogenous LC3 is a marker for autophagy. *Autophagy* 2005; **1**: 84–91.
18. Scarlatti F, Bauvy C, Ventruti A, Sala G, Cluzeaud F, Vandewalle A *et al.* Ceramide-mediated macroautophagy involves inhibition of protein kinase B and up-regulation of beclin 1. *J Biol Chem* 2004; **279**: 18384–18391.
19. Han W, Li L, Qiu S, Lu Q, Pan Q, Gu Y *et al.* Shikonin circumvents cancer drug resistance by induction of a necroptotic death. *Mol Cancer Ther* 2007; **6**: 1641–1649.
20. Nicholson DW, Ali A, Thornberry NA, Vaillancourt JP, Ding CK, Gallant M *et al.* Identification and inhibition of the ICE/CED-3 protease necessary for mammalian apoptosis. *Nature* 1995; **376**: 37–43.
21. Rudel T, Bokoch GM. Membrane and morphological changes in apoptotic cells regulated by caspase-mediated activation of PAK2. *Science* 1997; **276**: 1571–1574.
22. Devarajan E, Sahin AA, Chen JS, Krishnamurthy RR, Aggarwal N, Brun AM *et al.* Down-regulation of caspase 3 in breast cancer: a possible mechanism for chemoresistance. *Oncogene* 2002; **21**: 8843–8851.
23. Woo M, Hakem R, Soengas MS, Duncan GS, Shahinian A, Kagi D *et al.* Essential contribution of caspase 3/CPP32 to apoptosis and its associated nuclear changes. *Genes Dev* 1998; **12**: 806–819.
24. Kagawa S, Gu J, Honda T, McDonnell TJ, Swisher SG, Roth JA *et al.* Deficiency of caspase-3 in MCF7 cells blocks Bax-mediated nuclear fragmentation but not cell death. *Clin Cancer Res* 2001; **7**: 1474–1480.
25. Paglin S, Lee NY, Nakar C, Fitzgerald M, Plotkin J, Deuel B *et al.* Rapamycin-sensitive pathway regulates mitochondrial membrane potential, autophagy, and survival in irradiated MCF-7 cells. *Cancer Res* 2005; **65**: 11061–11070.
26. Kim KW, Mutter RW, Cao C, Albert JM, Freeman M, Hallahan DE *et al.* Autophagy for cancer therapy through inhibition of pro-apoptotic proteins and mammalian target of rapamycin signaling. *J Biol Chem* 2006; **281**: 36883–36890.
27. Cao C, Subhawong T, Albert JM, Kim KW, Geng L, Sekhar KR *et al.* Inhibition of mammalian target of rapamycin or apoptotic pathway induces autophagy and radiosensitizes PTEN null prostate cancer cells. *Cancer Res* 2006; **66**: 10040–10047.
28. Moretti L, Attia A, Kim KW, Lu B. Crosstalk between Bak/Bax and mTOR signaling regulates radiation-induced autophagy. *Autophagy* 2007; **3**: 142–144.
29. Hsieh TC, Burfeind P, Laud K, Backer JM, Traganos F, Darzynkiewicz Z *et al.* Cell cycle effects and control of gene expression by resveratrol in human breast carcinoma cell lines with different metastatic potentials. *Int J Oncol* 1999; **15**: 245–252.
30. Scifo C, Cardile V, Russo A, Consoli R, Vancheri C, Capasso F *et al.* Resveratrol and propolis as necrosis or apoptosis inducers in human prostate carcinoma cells. *Oncol Res* 2004; **14**: 415–426.
31. Zhu JH, Horbinski C, Guo F, Watkins S, Uchiyama Y, Chu CT. Regulation of autophagy by extracellular signal-regulated protein kinases during 1-methyl-4-phenylpyridinium-induced cell death. *Am J Pathol* 2007; **170**: 75–86.
32. Yano K, Hattori M, Moriyasu Y. A novel type of autophagy occurs together with vacuole genesis in miniprotoplasts prepared from tobacco culture cells. *Autophagy* 2007; **3**: 215–221.
33. Pattingre S, Tassa A, Qu X, Garuti R, Liang XH, Mizushima N *et al.* Bcl-2 antiapoptotic proteins inhibit Beclin 1-dependent autophagy. *Cell* 2005; **122**: 927–939.
34. Chan EY, Kir S, Tooze SA. siRNA screening of the kinome identifies ULK1 as a multidomain modulator of autophagy. *J Biol Chem* 2007; **282**: 25464–25474.
35. Vandenabeele P, Vanden Berghe T, Festjens N. Caspase inhibitors promote alternative cell death pathways. *Sci STKE* 2006; **2006**: pe44.
36. Faraglia B, Bonsignore A, Scaldaferri F, Boninsegna A, Cittadini A, Mancuso C *et al.* Caspase-3 inhibits the growth of breast cancer cells independent of protease activity. *J Cell Physiol* 2005; **202**: 478–482.
37. Howitz KT, Bitterman KJ, Cohen HY, Lamming DW, Lavu S, Wood JG *et al.* Small molecule activators of sirtuins extend *Saccharomyces cerevisiae* lifespan. *Nature* 2003; **425**: 191–196.
38. Meley D, Bauvy C, Houben-Weerts JH, Dubbelhuis PF, Helmond MT, Codogno P *et al.* AMP-activated protein kinase and the regulation of autophagic proteolysis. *J Biol Chem* 2006; **281**: 34870–34879.
39. Kueck A, Opipari Jr AW, Griffith KA, Tan L, Choi M, Huang J *et al.* Resveratrol inhibits glucose metabolism in human ovarian cancer cells. *Gynecol Oncol* 2007; **107**: 450–457.
40. Pattingre S, Petiot A, Codogno P. Analyses of Galpha-interacting protein and activator of G-protein-signaling-3 functions in macroautophagy. *Methods Enzymol* 2004; **390**: 17–31.

Supplementary Information accompanies the paper on Cell Death and Differentiation website (http://www.nature.com/cdd)